Mapping the Danish Business Cycle

Advanced Empirical Macroeconomic Analysis

Martin A. Kildemark*

December 2024

Abstract

In this paper, I map the Danish business cycle by estimating unobserved cycles and trends. I do this using two series of real GDP observations: a quarterly series from 1991Q1 to 2024Q2 and an annual series from 1870 to 2023. I find that troughs in the output gap on average occur around 3% below trend, while peaks occur around 2.3% above trend, with both peaks and troughs generally being larger in the historical dataset. The average duration from trough to peak is around twice the duration from peak to trough, with troughs typically occurring 3 years after a peak, while peaks occur 5.5 years after a trough. I find an annual trend growth of around 2.5%, but with a significant and prolonged decline around the financial crisis from 2006 to 2015 and during the 1930s.

*University of Copenhagen

Contents

1 Introduction **3**

2 Related Literature **4**

3 Defining the Business Cycle **5**

4 Estimating Trends and Cycles **7**

4.1 The Model 7

4.2 Estimation 9

5 Results **10**

6 Cycle Characteristics **13**

7 Discussion **16**

8 Conclusion **17**

A Estimation and Results **21**

A.1 Posteriors, Priors and Trace Plots 21

A.2 Estimation Algorithm 21

B Econometric Background **23**

B.1 State Space Models and the Kalman Filter 23

B.2 Bayesian Estimation 25

1 Introduction

Knowledge of past business cycles, and how they evolve, is valuable for policymakers when assessing stabilization policies and the general evolution of economic growth and volatility. When conducting stabilization policies, knowledge of economic fluctuations and trends is crucial, but these cannot be observed directly in economic data. As such, policies are based on estimates of the state of the economy, and methods that can provide these estimates are needed.

In this paper, I map past Danish business cycles by dissecting real GDP into a trend component and a cyclical component. I do this by formulating a time series model, which I estimate using Bayesian methods. I define how the business cycle is interpreted in this paper and discuss different interpretations of the cycle. By applying a trend-cycle model, I use an interpretation comparable to structural macroeconomic models analyzing output gaps as deviations from a steady state or structural level. These models are often used when discussing short-run dynamics between real and nominal variables, e.g., through a Phillips curve and optimal stabilization policies. I compare the estimated cycle to business cycles obtained when defining the business cycle as recessionary periods in aggregate activity, as done by the NBER and the CEPR, who date business cycles for the US and the euro area, respectively.

I estimate the model using seasonally adjusted quarterly real GDP from 1991 to 2024. My estimation results show that fluctuations in output are predominantly caused by transitory shocks with low persistence. The estimated trend is smooth and zero persistence "noise" shocks are small. The quarterly trend growth is generally around 0.5% per quarter except for the period 2006-2015. In this period, the trend is stagnating and even declining in 2008-2009. I identify four troughs and four peaks in the cycle. The troughs are generally deeper than the peaks are high and the duration from peak to trough is significantly shorter than the duration from trough to peak indicating a skewness in the business cycle. This skewness has long been acknowledged and already observed in Mitchell (1927), who observed how busts are large and happen quickly compared to booms. All the identified troughs in the cycle occur just after a recessionary period in aggregate activity.

I also analyze the Danish business cycle from a historical perspective using annual real GDP data dating back to 1870. The skewness in the business cycle is still evident, and cycles are on average larger, especially driven by very large movements from 1914 to 1950, with the two world wars causing negative output gaps of around 15% and low trend growth through the 1930s. Trend growth was generally around 3% per year before the 1950s, which saw trend growth of over 4% per year until the mid-1960s. From the 1970s, trend growth has been around 2% per year, with a clear prolonged drop around the financial crisis.

2 Related Literature

I estimate trends and cycles using a linear univariate time series model as in Harvey and Trimbur (2003). The model is an elaboration of the unobserved components model introduced in Watson (1986) where GDP observations are given by an unobserved stochastic trend and a stationary stochastic cycle. Harvey et al. (2007) expands the model in Harvey and Trimbur (2003) to the multivariate setting to study how other variables such as consumption, investments or inflation may be used to estimate trends and cycles in aggregate output. This multivariate settinghas been applied in recent work such as Hasenzagl et al. (2022), who formulate a model incorporating a Phillips curve, long-run expectations, and energy price shocks in the business cycle to model how they believe the central banks view inflation. Jarociński and Lenza (2018) uses similar methods to estimate a trend and cycle in GDP consistent with observed inflation following the financial crisis.

Morley et al. (2003) considers the classical unobserved components model from Watson (1986), which assumes that disturbances to the trend and cycle are uncorrelated. When allowing for correlation between these disturbances, Morley et al. (2003) find that they are negatively correlated, and both the trend and cycle are characterized by frequent fluctuations, with cycles bearing no resemblance to recessionary periods identified by the NBER. Grant and Chan (2017) and Perron and Wada (2009) consider these noisy trend and cycle estimates, which are at odds with intuition about trends and cycles. Perron and Wada (2009) find that a non-stochastic trend with time-varying drift circumvents the issue and results in trends and cycles in accordance with identified recessions and classical filtering

methods. They find that the non-stochastic trend is supported by their data set. Grant and Chan (2017) do not rely on a non-stochastic trend, but show that formulating the trend as a second-order Markov process also results in meaningful cycles and trends while allowing for disturbances in the trend to be correlated with the cycle. The model proposed in Harvey and Trimbur (2003), which is used in this paper, incorporates a stochastic time-varying drift, but the trend itself is non-stochastic given the drift, as in Perron and Wada (2009).

These models are all linear and therefore assume the cycle is mean-zero. Hamilton (1989) considers a cycle in a regime switching model allowing for nonlinearities. This paved the way for researchers to analyze differences between booms and busts in the economy. Kim and Nelson (1999) use a Markov-switching unobserved components model and find evidence of Friedman's plucking hypothesis: output moves along a ceiling given by a structural level, and is at times plucked down resulting in asymmetric fluctuations in output. Similar approaches are taken in Morley and Piger (2012), who find small positive cycles in expansions and large negative cycles in recessions. Kim et al. (2005) find that cycles are generally characterized by a sharp decline in output, a fast recovery, and then a stable period until the next decline. As such, cycles can be imagined as downward pointing triangles. This tendency is also found in Sichel (1994) when looking at aggregate data and not considering trend-cycle decompositions. These asymmetric characteristics indicate much larger welfare costs of business cycles than those found in Lucas Jr (2003), who assumes symmetric cycles around the trend. These nonlinear results are obtained from interpretations of estimated model parameters. Obtaining proper estimates of the unobserved cycles and trends is challenging in the nonlinear case, as estimates can no longer be based on the full information set using the Kalman smoother. As such, the research using nonlinear models provides an interesting discussion on business cycle dynamics and how optimal policy may vary depending on how cycles are characterized, but in this paper I rely on the linear model to obtain estimates of past cycles and trends.

3 Defining the Business Cycle

The term *"business cycle"* is a key concept in macroeconomics, but no clear-cut definition exists. Two common but different interpretations of business cycles are discussed in Morley and Piger (2012), who distinguish between an *"alternating-phases"* interpretation and an

"output gap" interpretation:

- *alternating-phases*: The alternation between persistent phases of increasing and stagnating or stalling aggregate economic activity
- *output gap*: The transitory fluctuations around a structural or trend level of output

The first interpretation is adopted by the NBER and CEPR when dating business cycles. The second interpretation is a more structural view of the business cycle. This interpretation is comparable to the output gaps often analyzed in DSGE models. How does the economy fluctuate around a natural/structural level? Morley and Piger (2012) argue that this makes the output gap interpretation more useful and relevant both in a theoretical sense and for policymakers. Harding and Pagan (2002) argue that business cycles should not be identified using estimated trends and output gaps, as they rely on the model or filter used and sometimes yield unintuitive results that diverge heavily from the cycles estimated by the NBER.

I apply the output-gap interpretation of the business cycle in this paper, but I compare the estimated cycle to recessionary periods as identified by the NBER and CEPR. This comparison between estimated cycles from trend-cycle decompositions and NBER business cycles is common and is also used in Morley and Piger (2012) and Antolin-Diaz et al. (2017). I identify the recessionary periods in Denmark using a quarterly Bry & Boschan algorithm presented in Harding and Pagan (2002), which aligns the turning-point identification method from Bry and Boschan (1971) with quarterly data.[1] The same method is used by the Danish central bank in Haugaard Jensen and Jensen (2019), who argue that these estimated recessions can be seen as a Danish equivalent to the NBER and CEPR recessions. The identified recessionary periods are seen in Figure 1.

[1] I use the BBQ package in R to identify recessionary periods

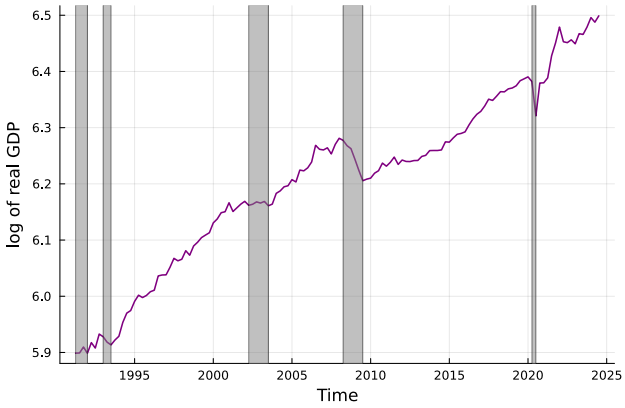

Figure 1: Recessionary Periods in Denmark

Note: Grey bands show recessionary periods estimated using the Bry & Boschan algorithm. An identified recessionary period in 2006 and in 2022 is removed following Haugaard Jensen and Jensen (2019), due to no recessionary signs in unemployment.

4 Estimating Trends and Cycles

To estimate the cycles and trend in economic activity in Denmark, I formulate a time series model as in Harvey and Trimbur (2003).

4.1 The Model

Observations y_t are assumed to consist of a trend component μ_t, a cyclical component ψ_t and residual noise ϵ_t:

$$y_t = \mu_t + \psi_{n,t} + \epsilon_t, \quad \epsilon_t \sim \mathcal{N}(0, \sigma_\epsilon).$$

The trend is modeled as non-stochastic at t conditional on $t-1$ but with a stochastic drift following a random walk:

$$\begin{aligned} \mu_t &= \mu_{t-1} + \beta_{t-1} \\ \beta_t &= \beta_{t-1} + \xi_t, \quad \xi_t \sim \mathcal{N}(0, \sigma_\xi). \end{aligned}$$

This trend formulation allows for time-varying trend growth compared to stochastic trends modeled as a random walk with constant drift, where trend growth fluctuates around a fixed mean. This allows the model to capture decreases or increases in trend growth, but it implies

that the growth rate in y_t is integrated of order 2 and therefore not stationary when taking first differences. This implies that the growth rate in y_t can drift without bound. This is an unrealistic assumption, but nevertheless harmless as long as the variance of the drift σ_ξ is small and the period considered is finite as discussed in Antolin-Diaz et al. (2017). An alternative approach used in Perron and Wada (2009) is to model the trend with a deterministic drift, but allow for and locate break-points in the drift.

The cycle is modeled as an n^{th}-order cycle. Harvey and Trimbur (2003) show that the use of higher-order cycles results in smoother cycle estimates, making analysis of peaks and troughs easier. The cycle is formulated as:

$$\begin{pmatrix} \psi_{1,t} \\ \psi^*_{1,t} \end{pmatrix} = \rho \begin{pmatrix} \cos\lambda_c & \sin\lambda_c \\ -\sin\lambda_c & \cos\lambda_c \end{pmatrix} \begin{pmatrix} \psi_{1,t-1} \\ \psi^*_{1,t-1} \end{pmatrix} + \begin{pmatrix} \kappa_t \\ \kappa^*_t \end{pmatrix}$$

$$\begin{pmatrix} \psi_{n,t} \\ \psi^*_{n,t} \end{pmatrix} = \rho \begin{pmatrix} \cos\lambda_c & \sin\lambda_c \\ -\sin\lambda_c & \cos\lambda_c \end{pmatrix} \begin{pmatrix} \psi_{n,t-1} \\ \psi^*_{n,t-1} \end{pmatrix} + \begin{pmatrix} \psi_{n-1,t-1} \\ \psi^*_{n-1,t-1} \end{pmatrix}$$

with $\kappa_t \sim \mathcal{N}(0, \sigma_\kappa)$ and $\kappa^*_t \sim \mathcal{N}(0, \sigma_\kappa)$. I apply a 2nd order cycle, $n = 2$. The model then consists of the parameter vector $\theta = (\rho, \lambda_c, \sigma_\epsilon, \sigma_\xi, \sigma_\kappa)$ and the unobserved states vector $\alpha = (\mu, \beta, \psi_1, \psi^*_1, \psi_2, \psi^*_2)$ where μ and ψ_2 are the states of special interest. Parameter estimates also contain interesting insights about how the economy fluctuates. The variance parameters contain information about which type of shocks generate fluctuations. If σ_ϵ is relatively large, fluctuations are driven by zero-persistence noise shocks. If σ_ξ is relatively large, fluctuations are driven by permanent shocks and if σ_κ is relatively large fluctuations are driven by transitory cyclical shocks. The functional form of the cycle results in these cyclical shocks generating ripple waves around zero following the shock, where λ_c is the frequency of the wave structure in radians and ρ is a damping factor allowing the ripple waves to decay over time. If $\lambda_c = \pi$, it will take the cycle one period to go from a peak to a trough if affected by no other shocks while if $\lambda_c = \pi/2$, it will take two periods.

4.2 Estimation

To estimate the model, I formulate it in the state space form and use Bayesian methods to estimate the distributions of model parameters and unobserved states. Harvey et al. (2007) estimate the same model on US data using Bayesian methods, but I follow an approach similar to Hasenzagl et al. (2022). I apply a Markov Chain Monte Carlo algorithm where model parameters are sampled from their posterior distribution using Metropolis-Hastings sampling, and unobserved states are sampled using Gibbs sampling by applying the simulation smoother suggested in Durbin and Koopman (2002). The applied algorithm is outlined in appendix A.2, and state space models as well as the applied Bayesian methods, are explained in appendix B. I implement the estimation algorithm using the Julia programming language by Bezanson et al. (2017).[2] When using Bayesian methods, prior beliefs about the distribution of parameters can be included. I do not include any prior beliefs and use uninformative priors given by the uniform distribution, but I bound the parameters in their support. I do this as a variance must be positive, and ρ must be lower than 1 for the cycle to be stationary. The prior distributions and support of the parameters are shown in table 1 below.

Name	**Support**	**Density**	**Parameter 1**	**Parameter 2**
σ^2	$(0, \infty)$	Uniform	10^{-6}	10^6
ρ	$[0.001, 0.99]$	Uniform	0.001	0.99
λ_c	$[0.001, \pi]$	Uniform	0.001	π

Table 1: Prior Distributions

I estimate the model on two series of Danish GDP data. The first series consists of seasonally adjusted quarterly observations of real GDP from 1991Q1 to 2024Q2. The second series consists of annual real GDP observations dating back to 1870 and is constructed using multiple data sources. I use an initial estimate of nominal GDP in 1870 and construct the series using annual real growth rates. From 1870 to 1929, observations of real growth rates are historical estimates obtained from Hansen (1972). From 1930 to 2023, real growth rates

[2] All files used to generate results are available at https://github.com/MKildemark/State-Space-Model-Estimation

are obtained from the official Danish national accounts. The series are log-transformed, so the estimated cycle can be interpreted as an approximate percentage deviation from trend. Both series are plotted in Figure 2.

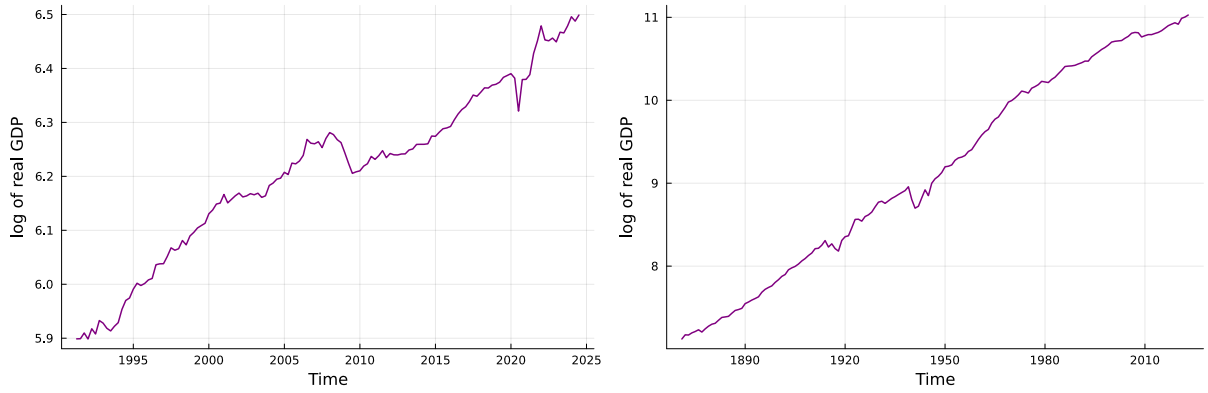

(a) Quarterly GDP Series

(b) Historical Annual GDP Series

Figure 2: Data

5 Results

The posterior means of the estimated parameters are shown in Table 2 below. The full posterior distributions are seen in Figure 9 in the appendix. The posteriors have defined peaks away from zero, indicating that they are identified in the data, but a lot of probability mass is still at the lower bounds for λ_c and σ_ξ. The damping factor ρ and frequency λ_c are similar across both data series, which is surprising, considering one series is quarterly data and one is annual data. λ_c is estimated to be small around 0.1 for both series. This means that, absent other shocks, it will take the cycle 30 periods (quarters/years) to go from a peak to a trough, while the damping factor of around 0.5 implies that the cycle has decayed to just 1/16 of its original size after four periods. As such, a transitory shock is not very persistent and almost fully gone after a year for the quarterly estimates. Such a shock in itself does not create noticeable waves or ripple effects. The notion that a positive transitory shock today will cause a negative output gap at some point in the future is therefore not seen in the data. The estimates from the quarterly series are comparable with those found in Harvey et al. (2007), who estimates the model on quarterly US data from 1947 to 2005. They also find low-frequency cycles, but with slightly more persistence with ρ around 0.7. For both series, the variance is highest among disturbances to the cycle, σ_κ, and significantly lower for

disturbances to the trend σ_ξ. This indicates that fluctuations in economic output are caused by transitory shocks, and to some degree noise through σ_ϵ, but not through permanent shocks. This is also the case in Harvey et al. (2007). Morley et al. (2003) argue that this is common in unobserved components models, but not the case when allowing for a stochastic trend with disturbances correlated with those of the cycle. Then the trend becomes volatile and the cycle essentially looks like noise. Much of the literature on nonlinear cycles, like Morley and Piger (2012), Kim et al. (2005) and Kim and Nelson (1999), find that fluctuations are driven by permanent shocks in expansionary times, but large transitory shocks during contractions.

Table 2: MCMC Parameter Estimates

	1991Q1–2024Q2	**1870–2023**
ρ	0.524	0.492
λ_c	0.100	0.119
σ_ξ^2	4.089×10^{-6}	2.936×10^{-5}
σ_κ^2	6.0167×10^{-5}	7.868×10^{-4}
σ_ϵ^2	4.008×10^{-5}	1.267×10^{-4}

Note: Parameter estimates are given by the mean of the posterior distribution. Full posterior distributions are shown in Figure 9 in the appendix

The estimated trend, cycle, trend growth and noise (residuals) for the quarterly series are shown in Figures 3 and 4 below. The financial crisis and COVID-19 are noticeable in the cycle, with these periods being the only periods with 95% credible intervals below zero. Subfigure 4a shows how trend growth is usually around or slightly above 0.5% per quarter, but with a large slump around the financial crisis. It decreases during 2006, and even becomes negative in 2008. Trend growth only returns to 0.5% per quarter again in 2015. This prolonged decline in trend growth around the financial crisis is also found in Hasenzagl et al. (2022) and Antolin-Diaz et al. (2017) for the US and in Jarociński and Lenza (2018) for the euro area using multivariate models. The decrease in trend growth is larger in my estimates, however, while the negative output gap around the financial crisis is less persistent and already closed by 2011. In contrast, it persists until 2017 in Hasenzagl et al. (2022) and beyond 2015 in Jarociński and Lenza (2018). Coibion et al. (2017) argue that trend estimates in such unobserved components models and more structural DSGE models can be

affected by shocks that have no long-run effects on output. They therefore argue that the estimated decline in trend growth during the financial crisis, as seen in my results, might be exaggerated.

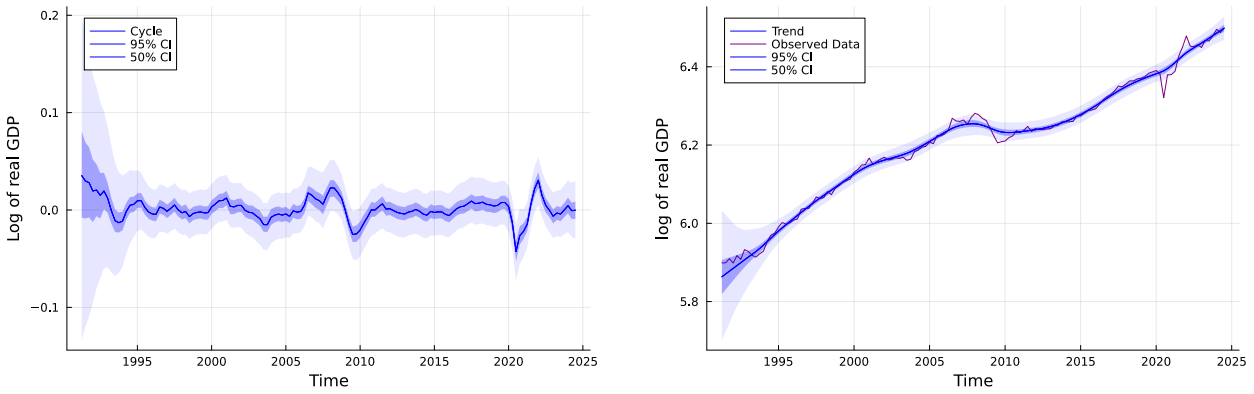

(a) Cycle (b) Trend

Figure 3: Estimated Cycle and Trend 1991Q1-2024Q2

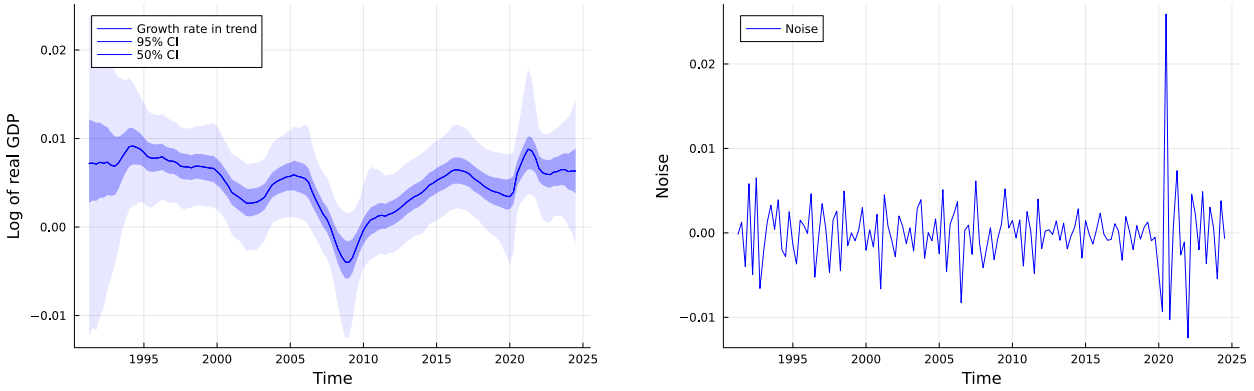

(a) Trend Growth (b) Noise

Figure 4: Trend Growth and Noise 1991Q1-2024Q2

The estimated trend and cycle from the annual series from 1870 to 2023 are shown in Figures 5 and 6 below. The cycle is no longer significantly negative during the financial crisis and COVID-19, but only during the two world wars, where output is more than 15% below trend. The insignificant cycle is most likely caused by the low frequency of observations, and highlights how annual data is not ideal when studying short-run economic fluctuations. The estimates do, however, provide interesting historical insights about the Danish economy. Up until the First World War, fluctuations in the cycle were frequent but not large. The period 1918-1950 is characterized by large fluctuations in the output gap in the range of around

-18% to 10%. After 1950, output gaps are generally larger and smoother than before 1918, and much smaller than 1918-1950. Trend growth is around 3% per year until the 1930s, where it slumps. After the Second World War, trend growth increases heavily and is around 4% through the 1950s and 1960s before decreasing in the 1970s. The prolonged slump around the financial crisis is also visible, but the decrease is less than in the quarterly series, leading to a more prolonged negative output gap after the financial crisis—more comparable with estimates from other studies like Hasenzagl et al. (2022), as discussed previously.

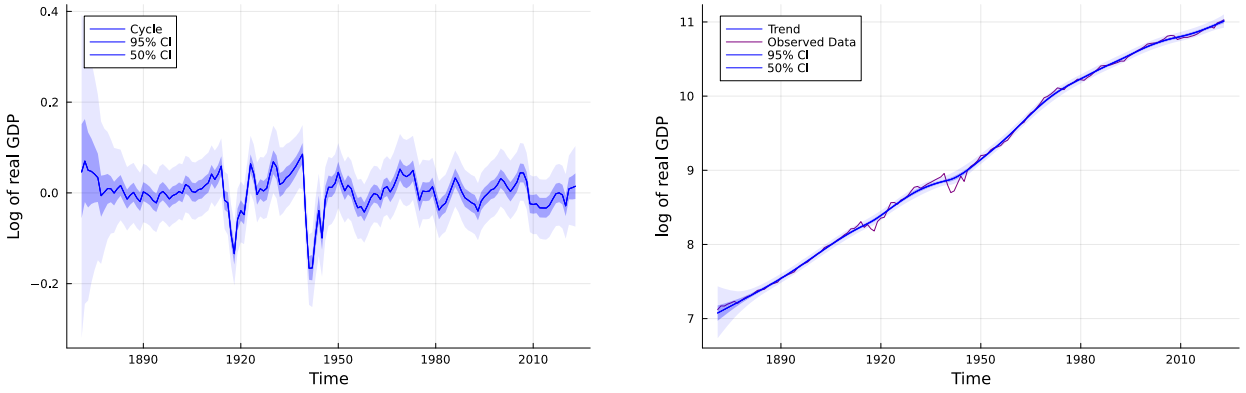

(a) Cycle (b) Trend

Figure 5: Estimated Historical Cycle and Trend 1870-2023

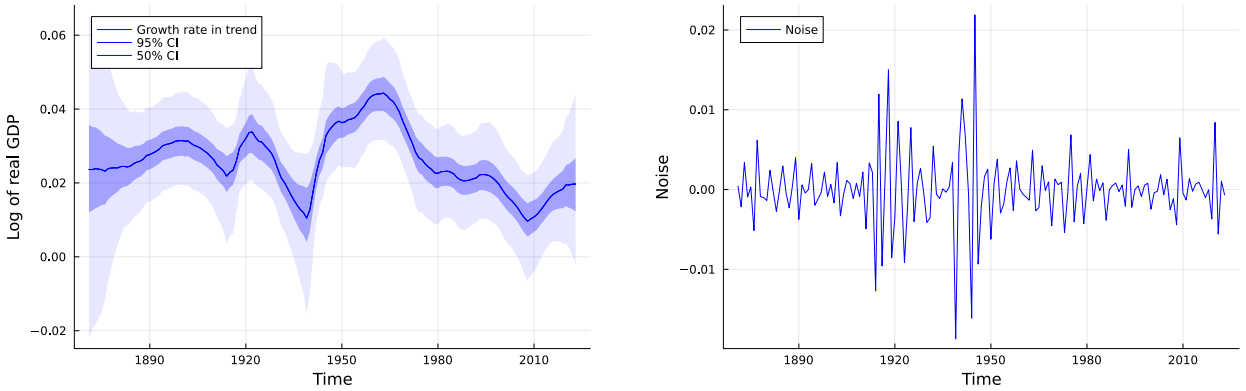

(a) Trend Growth (b) Noise

Figure 6: Trend Growth and Noise 1870-2023

6 Cycle Characteristics

In this section, I quantify some characteristics of the estimated Danish business cycle. To do this, I locate peaks and troughs in the cycles. In the quarterly series, I define troughs

as the minimum value of the cycle in sections where it is significantly negative at the 50% confidence level. Peaks are then located as the maximum level of the cycle after a trough. Because of the general insignificance of the cycle in the annual series, this method is only suitable for the quarterly series. For the annual series, I locate all points where the cycle crosses zero. Between each zero-crossing there must be a peak or a trough, which I find by locating the largest absolute deviation from zero between the zero-crossings. The located peaks and troughs are displayed in Figure 7, where estimated recessionary periods are also reported for the quarterly series in panel 7a. Peaks and troughs are also reported in Table 3. All peaks and troughs in the quarterly series are also located in the annual series except for the peak around the end of 2000 and the trough at the end of 2003. The trough from the financial crisis is also identified in 2014 instead of 2009.

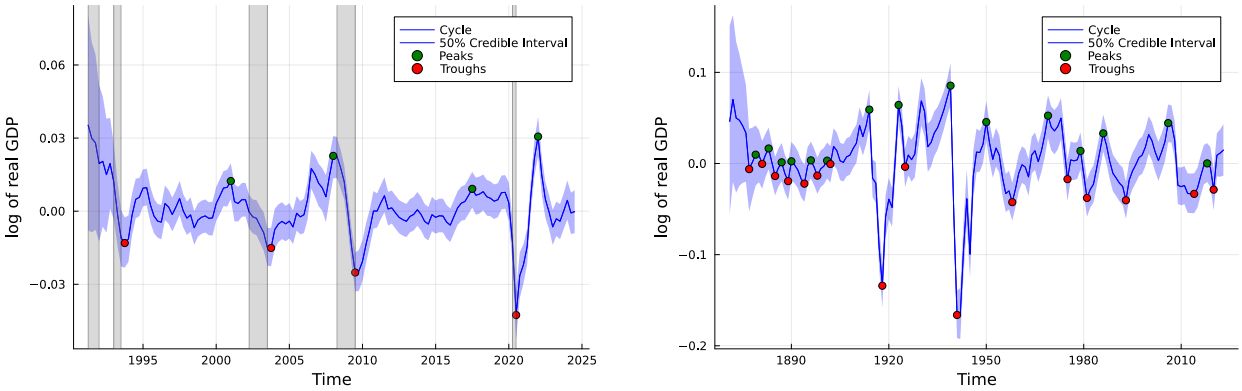

(a) 1991- (b) 1870-

Figure 7: Estimated Peaks and Troughs

Note: Figures show identified peaks and troughs in estimated cycles. Grey bands in panel a) indicate recessionary periods identified using the Bry-Boschan algorithm.

Table 3: Peaks and Troughs

1991Q1-2024Q2
Peaks: 2000Q4, 2007Q4, 2017Q2, 2021Q4
Troughs: 1993Q3, 2003Q3, 2009Q2, 2020Q2
1870-2023
Peaks: 1879, 1883, 1887, 1890, 1896, 1901, 1914, 1923, 1939.0, 1950, 1969, 1979, 1986, 2006, 2018
Troughs: 1877, 1881, 1885, 1889, 1894, 1898, 1902, 1918, 1925, 1941, 1958, 1975, 1981, 1993, 2014, 2020

Each identified trough in the quarterly series is located at the end of a recessionary period

indicating a strong link between the *output gap* and *alternating phases* view of the business cycle. Harding and Pagan (2002) are critical of the output gap view, as they argue that different trend-cycle decompositions may give unintuitive and very different results with no link to what is experienced as recessionary periods in the real world. In Figure 8, cycles are compared to cycles obtained using common trend-cycle filtering methods: the Hodrick-Prescott filter and the Butterworth filter. The estimated cycles are very similar to those obtained from the filters, except for the initial periods where the estimated cycles are large and positive with very wide credible intervals as seen above. As such, the critique of trend-cycle decompositions in Harding and Pagan (2002) seems too harsh, as also suggested in Morley and Piger (2012). The estimated cycles are intuitive and in line with real-world events and what would be expected.

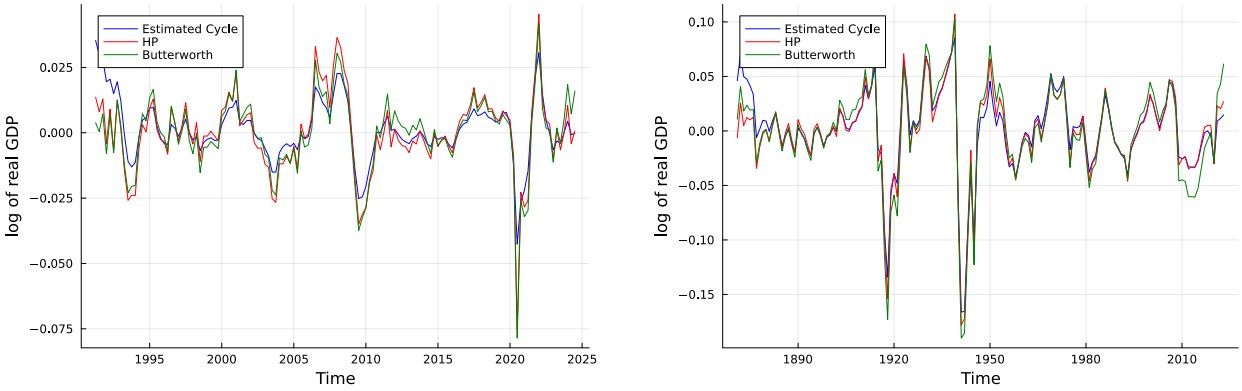

(a) 1991Q1-2024Q2 (b) 1870-2023

Figure 8: Cycle Compared with Filter Based Estimates

Table 4 shows statistics about amplitudes and durations between the estimated peaks and troughs of the cycle. The cycles are mean-zero by assumption. The characteristics are comparable across both the quarterly series and the historical annual series. Troughs are generally deeper than peaks are high, and troughs occur shortly after a peak, while the distance from troughs to peaks is longer. As such, the cycle decreases quickly but seems to increase slowly. When looking at the estimated cycles it seems that troughs are deep and occur suddenly, but are followed by a quick increase back towards the trend level. After this rebound the cycle seems to stabilize at the trend, or increase at a slower rate until a new decline occurs. The exception seems to be the recovery after COVID-19, where the sharp rebound overshoots the trend and creates a large positive output gap. This rebound effect is also found in nonlinear models such as Kim et al. (2005) and in models not relying on

trend-cycle decompositions such as Sichel (1994). This nonlinear rebound effect cannot be tested or confirmed in this linear model, and can only be discussed qualitatively.

Table 4: Characteristics of the estimated cycles

Measure	**1991-**	**1870-**
Mean Trough-to-Peak Duration	5.3	5.9
Mean Peak-to-Trough Duration	2.4	3.7
Mean Peak-to-Peak Duration	7.0	9.9
Mean Trough-to-Trough Duration	8.9	9.5
Mean Expansion Amplitude	0.019	0.028
Mean Contraction Amplitude	-0.024	-0.036
Years with Significantly Positive Cycle	5.25	33
Years with Significantly Negative Cycle	3.75	30

Note: Duration is measured in years and amplitude is in logs (approximate percent deviation from trend). Significance is at the 50% credible level

7 Discussion

As seen in Figure 8, the estimated cycle is very similar to the cycles obtained from the Hodrick-Prescott filter and Butterworth filter, with these filters being much simpler to implement. So why even use a more complicated model with parameters to be estimated? The reason is the flexibility the time series models provide and the information the parameter estimates contain. In this paper, I only consider the univariate linear case, but the results have been related to papers applying multivariate models and nonlinear models. The multivariate models can be used to shed light on the business cycle, but also how other variables are affected by and affect the business cycle. The nonlinear models allow for a cycle that is not mean-zero and can behave very differently in different scenarios such as declines and expansions. Such models have been used to show that the business cycle is not symmetric around the trend, and that deviations above trend may be rare while deviations below trend may be more severe than the linear view of the business cycle implies.

In this paper, the focus has been on the univariate linear model to obtain optimal estimates

of the trend and cycle in Danish economic activity. In the univariate case, information from other series that may be relevant is not considered, but the inclusion of such series would also imply a range of assumptions about how these series should be included in the model. The identifying assumptions are, however, minimal compared to DSGE models. Hasenzagl et al. (2022) therefore calls such a multivariate model a semi-structural model that occupies the middle ground between VAR models and DSGE models. Since business cycles are seen as the fluctuations in aggregate economic activity, I only consider GDP data to map these fluctuations, and as such, impose minimal structure and assumptions at the cost of possibly ignoring informative data.

Nonlinear models have revealed asymmetries in business cycles, which have large implications for the costs of economic fluctuations and possibly for optimal economic policy as well. The policy implications of such nonlinearities have gained attention after the low GDP growth experienced following the financial crisis and the inflationary pressure experienced in the 2020s. These nonlinearities are studied in theoretical settings in Dupraz et al. (2019) and Benigno and Eggertsson (2023). They argue that these nonlinearities have large implications for optimal policies. Developing methods for reliably estimating unobserved trends and output gaps with nonlinearities present is a relevant goal for future research.

8 Conclusion

I have mapped the Danish business cycle by estimating unobserved trends and cycles in aggregate economic activity. From the estimated model parameters, I argue that fluctuations are driven by temporary shocks. These temporary shocks have low persistence and do not create ripple waves in future output, but decay quickly towards zero. I present the estimated cycles and trends, and argue that they are intuitive and closely linked with recessionary estimates comparable with those of the NBER and CEPR. The estimated troughs are generally deeper than the peaks are high. A trough occurs suddenly, but also creates a quick rebound effect afterwards, while peaks are created by a more steady increase in the cycle. The estimated trends show a significant slowdown in trend growth from 2006–2015, after which trend growth returns to levels comparable with the 1990s.

References

Antolin-Diaz, J., Drechsel, T., and Petrella, I. (2017). Tracking the slowdown in long-run gdp growth. *Review of Economics and Statistics*, 99(2):343–356.

Benigno, P. and Eggertsson, G. B. (2023). It's baaack: The surge in inflation in the 2020s and the return of the non-linear phillips curve. Technical report, National Bureau of Economic Research.

Bezanson, J., Edelman, A., Karpinski, S., and Shah, V. B. (2017). Julia: A fresh approach to numerical computing. *SIAM Review*, 59(1):65–98.

Bry, G. and Boschan, C. (1971). Cyclical analysis of time series: Selected procedures and computer programs. In *Cyclical analysis of time series: Selected procedures and computer programs*, pages 13–2. NBER.

Coibion, O., Gorodnichenko, Y., and Ulate, M. (2017). The cyclical sensitivity in estimates of potential output. Technical report, National Bureau of Economic Research.

Dupraz, S., Nakamura, E., and Steinsson, J. (2019). A plucking model of business cycles. Technical report, National Bureau of Economic Research.

Durbin, J. and Koopman, S. J. (2002). A simple and efficient simulation smoother for state space time series analysis. *Biometrika*, 89(3):603–616.

Grant, A. L. and Chan, J. C. (2017). Reconciling output gaps: Unobserved components model and hodrick–prescott filter. *Journal of Economic Dynamics and Control*, 75:114–121.

Hamilton, J. D. (1989). A new approach to the economic analysis of nonstationary time series and the business cycle. *Econometrica: Journal of the econometric society*, pages 357–384.

Hansen, S. A. (1972). Økonomisk vækst i danmark. *Københavns Universitet, Institut for Økonomisk Historie*.

Harding, D. and Pagan, A. (2002). Dissecting the cycle: a methodological investigation. *Journal of monetary economics*, 49(2):365–381.

Harvey, A. C. (1990). Forecasting, structural time series models and the kalman filter, chapter 3.

Harvey, A. C. and Trimbur, T. M. (2003). General model-based filters for extracting cycles and trends in economic time series. *Review of Economics and Statistics*, 85(2):244–255.

Harvey, A. C., Trimbur, T. M., and Van Dijk, H. K. (2007). Trends and cycles in economic time series: A bayesian approach. *Journal of Econometrics*, 140(2):618–649.

Hasenzagl, T., Pellegrino, F., Reichlin, L., and Ricco, G. (2022). A model of the fed's view on inflation. *Review of Economics and Statistics*, 104(4):686–704.

Haugaard Jensen, D. and Jensen, R. (2019). Heightened risk of a global recession.

Jarociński, M. and Lenza, M. (2018). An inflation-predicting measure of the output gap in the euro area. *Journal of Money, Credit and Banking*, 50(6):1189–1224.

Kim, C.-J., Morley, J., and Piger, J. (2005). Nonlinearity and the permanent effects of recessions. *Journal of Applied Econometrics*, 20(2):291–309.

Kim, C.-J. and Nelson, C. R. (1999). Friedman's plucking model of business fluctuations: tests and estimates of permanent and transitory components. *Journal of Money, Credit and Banking*, pages 317–334.

Lucas Jr, R. E. (2003). Macroeconomic priorities. *American economic review*, 93(1):1–14.

Mitchell, W. C. (1927). *Business Cycles: The Problem and Its Setting*. NBER.

Morley, J. and Piger, J. (2012). The asymmetric business cycle. *Review of Economics and Statistics*, 94(1):208–221.

Morley, J. C., Nelson, C. R., and Zivot, E. (2003). Why are the beveridge-nelson and unobserved-components decompositions of gdp so different? *Review of Economics and Statistics*, 85(2):235–243.

Perron, P. and Wada, T. (2009). Let's take a break: Trends and cycles in us real gdp. *Journal of monetary Economics*, 56(6):749–765.

Sichel, D. E. (1994). Inventories and the three phases of the business cycle. *Journal of Business & Economic Statistics*, 12(3):269–277.

Watson, M. W. (1986). Univariate detrending methods with stochastic trends. *Journal of monetary economics*, 18(1):49–75.

A Estimation and Results

A.1 Posteriors, Priors and Trace Plots

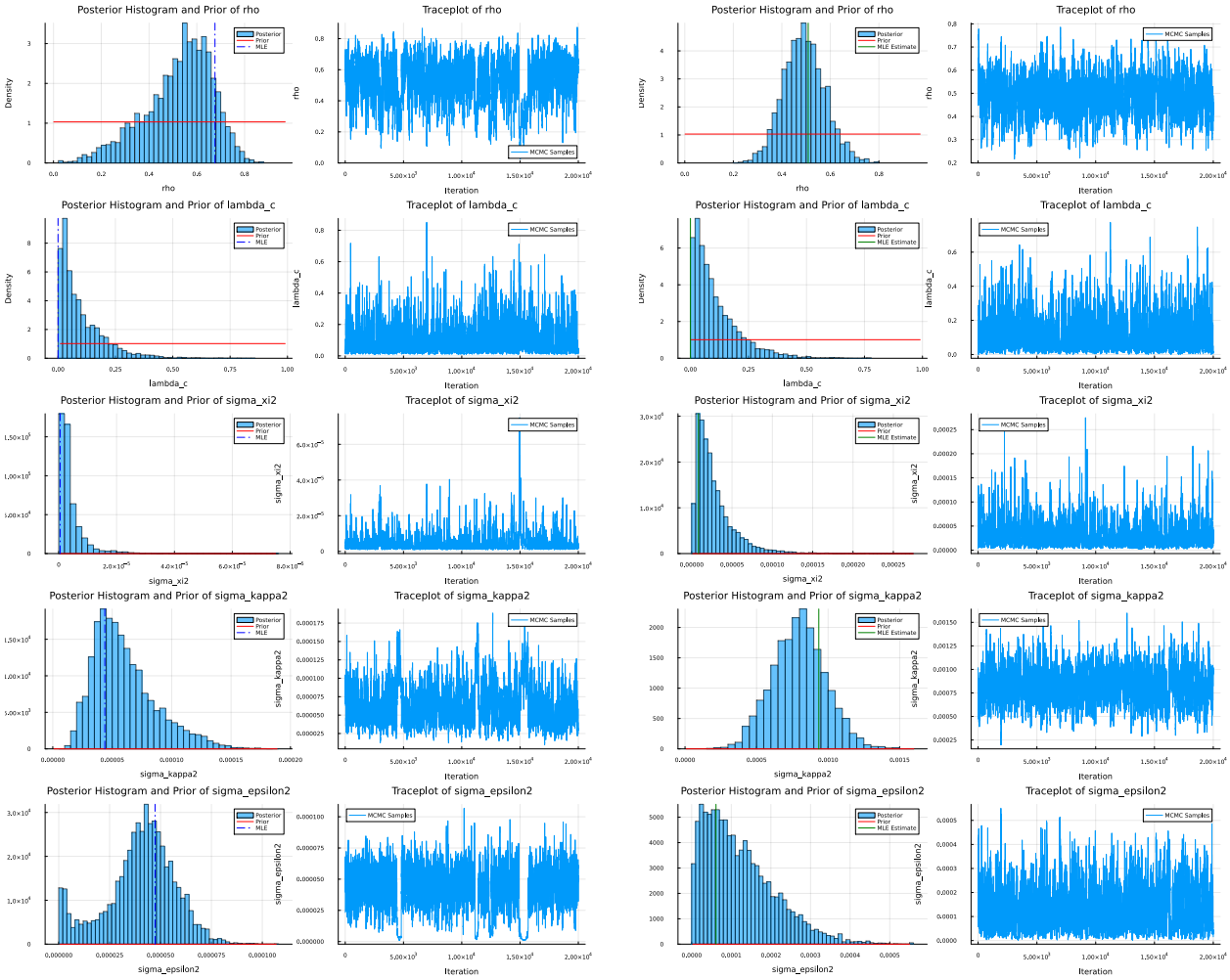

(a) 1991- (b) 1870-

Figure 9: Posteriors, Priors and Trace Plots

A.2 Estimation Algorithm

Initialization

For s = 1,..,40,000 draws:

Draw unbounded candidate vector Γ^* from multivariate normal distribution with mean Γ_{s-1} and variance-covariance ωI where ω is a scaling constant to get acceptance rate around 25-35 pct.

New draw is accepted with probability γ

$$\Gamma_s = \begin{cases} \Gamma_* & \text{with probability } \gamma \\ \Gamma_{s-1} & \text{with probability } 1-\gamma \end{cases}$$

where

$$\gamma = min\left(1, \frac{p(y|\theta^*)p(\theta^*)J(\Gamma^*)}{p(y|\theta_{s-1})p(\theta_{s-1})J(\Gamma_{s-1})}\right)$$

Where $J(\Gamma)$ are the Jacobians of the transformed variables: $\frac{d\theta}{d\Gamma}$.
First half of the initialization draws are discarded

Recursion

for q = 1,..., 40,000 draws:
Set Σ to sample covariance of the chain Γ_s from the initialization step. A candidate vector for the unbounded paramters Γ^* is drawn form a multivariate distribution with mean Γ_{q-1} and variance $\omega\Sigma$ with ω being a scaling constant to get 25-35 acceptance rate. New draw is accepted as in the initialization. Discard draws from burn in period.
For $q > 20,000$: After burn-in period sample unobserved states α using simulation smoother from Durbin and Koopman (2002)

Transformations and Jacobians

Parameters are bounded in their support, but drawn from an unbounded distribution. To get unbounded support the parameters are transformed using the following transformation:

$$\Gamma^{U,\beta} = \ln\left(\frac{\theta^{U,\beta} - a}{b - \theta^{U,\beta}}\right)$$

where a is the lower bound and b is the upper bound of their support. The inverse of the transformation is then

$$\theta^{U,\beta} = \frac{a + bexp(\Gamma^{U,\beta})}{1 + \exp(\Gamma^{U,\beta})}$$

and the log of the derivatives is

$$\ln\left(\frac{d\theta^{U,\beta}}{d\Gamma^{U,\beta}}\right) = \ln(b-a) + \Gamma^{U,\beta} - 2\ln(1+\exp(\Gamma^{U,\beta}))$$

B Econometric Background

B.1 State Space Models and the Kalman Filter

The State Space Form

In this section I provide a overview of Gaussian linear state space models. For more details see Harvey (1990). State Space Models are models where an $N \times 1$ outcome vector $\boldsymbol{y}_t$ is given by a set of underlying states $\boldsymbol{\alpha}_t$ through a *measurement equation* given by

$$\boldsymbol{y}_t = \boldsymbol{Z}\boldsymbol{\alpha}_t + \boldsymbol{d} + \boldsymbol{\epsilon}_t, \quad \boldsymbol{\epsilon}_t \sim \mathcal{N}(0, \boldsymbol{H}) \tag{1}$$

where $\boldsymbol{Z}$, $\boldsymbol{d}$ and $\boldsymbol{H}$ are non-stochastic. The states in the state-vector $\boldsymbol{\alpha}_t$ are generally not observable, but follow a first-order Markov process resulting in a *transition equation*

$$\boldsymbol{\alpha}_t = \boldsymbol{T}\boldsymbol{\alpha}_{t-1} + \boldsymbol{c} + \boldsymbol{R}\boldsymbol{\eta}_t, \quad \boldsymbol{\eta}_t \sim \mathcal{N}(0, \boldsymbol{Q}) \tag{2}$$

such that the expected states tomorrow are independent of all other states than the current. $\boldsymbol{c}$, $\boldsymbol{R}$ and $\boldsymbol{Q}$ are non-stochastic and are together with $\boldsymbol{Z}$, $\boldsymbol{d}$ and $\boldsymbol{H}$ referred to as the *system matrices*. These matrices are given by the structure and parameters $\boldsymbol{\theta}$ of the underlying model. The State Space model is closed with two final assumptions:

- There is an initial state vector with the distribution $\boldsymbol{\alpha}_0 \sim \mathcal{N}(\boldsymbol{a}_0, \boldsymbol{P}_0)$.
- Disturbances $\boldsymbol{\epsilon}_t$ and $\boldsymbol{\eta}_t$ are uncorrelated with each other and the initial state $\boldsymbol{\alpha}_0$ across all periods.

Once a model is formulated in this form it can be estimated using the *Kalman filter*.

The Kalman Filter

The Kalman filter is a recursive algorithm which provides the mean square error minimizing estimates of the state vector at time t given the available information at time t. This

information consists of the observed outcomes $\boldsymbol{y}_0, ..., \boldsymbol{y}_t$, together with the system matrices and the distribution of the initial states, $\boldsymbol{\alpha}_0 \sim \mathcal{N}(\boldsymbol{a}_0, \boldsymbol{P}_0)$, which are assumed to be known. The estimate of $\boldsymbol{\alpha}_t$ is denoted as $\boldsymbol{a}_t$, and $\boldsymbol{P}_t$ denotes the covariance matrix of the estimation error:

$$\boldsymbol{P}_{t-1} = E[(\boldsymbol{\alpha}_{t-1} - \boldsymbol{a}_{t-1})(\boldsymbol{\alpha}_{t-1} - \boldsymbol{a}_{t-1})'] \tag{3}$$

Given $\boldsymbol{a}_{t-1}$ and $\boldsymbol{P}_{t-1}$, the estimate of $\boldsymbol{\alpha}_t$ given available information at $t-1$ follows from the state space form at gives the *prediction equations*:

$$\boldsymbol{a}_{t|t-1} = \boldsymbol{T}\boldsymbol{a}_{t-1} + \boldsymbol{c} \tag{4}$$

$$\boldsymbol{P}_{t|t-1} = \boldsymbol{T}\boldsymbol{P}_{t-1}\boldsymbol{T}' + \boldsymbol{R}\boldsymbol{Q}\boldsymbol{R}' \tag{5}$$

Then at time t the observation of $\boldsymbol{y}_t$ becomes available and the state estimate is updated through the *updating equations*:

$$\mathbf{y}_{t|t-1} = \boldsymbol{Z}\boldsymbol{a}_{t|t-1} + \boldsymbol{d} \tag{6}$$

$$\boldsymbol{a}_t = \boldsymbol{a}_{t|t-1} + \boldsymbol{P}_{t|t-1}\boldsymbol{Z}'\boldsymbol{F}_t^{-1}(\boldsymbol{y}_t - \mathbf{y}_{t|t-1}) \tag{7}$$

$$\boldsymbol{P}_t = \boldsymbol{P}_{t|t-1} - \boldsymbol{P}_{t|t-1}\boldsymbol{Z}'\boldsymbol{F}_t^{-1}\boldsymbol{Z}\boldsymbol{P}_{t|t-1} \tag{8}$$

where

$$\boldsymbol{F}_t = \boldsymbol{Z}\boldsymbol{P}_{t|t-1}\boldsymbol{Z}' + \boldsymbol{H}$$

The updating equation intuitively works as follows: if $\boldsymbol{H}$ is large, observations are noisy, and the new observations $\boldsymbol{y}_t$ are weighted less when updating the state estimate, the the estimate relies more on the model structure. If $\boldsymbol{P}_{t|t-1}$ is large their is more uncertainty in the prediction $\boldsymbol{a}_{t|t-1}$ and the updated estimate relies more on the new observations.

Conditional on information available at time $t-1$ the estimate for $\boldsymbol{y}_t$ is given by $\mathbf{y}_{t|t-1}$ and the conditional variance is given by $\boldsymbol{F}_t$. As disturbances and the initial state vector are normal and independently distributed $\boldsymbol{y}_t$ is normal and independently distributed when

conditioned on $\boldsymbol{y}_{t-1}, ...\boldsymbol{y}_1$. The likelihood function is then given by

$$L(\boldsymbol{\theta}|\boldsymbol{y}) = \prod_{t=1}^{T} p(\boldsymbol{y_t}|\boldsymbol{y}_{t-1}, ...\boldsymbol{y}_1) \tag{9}$$

$$\Leftrightarrow logL = -\frac{NT}{2}log2\pi - \frac{1}{2}\sum_{t=1}^{T} log|\boldsymbol{F}_t| - \frac{1}{2}\sum_{t=1}^{T} \boldsymbol{v}_t'\boldsymbol{F}_t^{-1}\boldsymbol{v}_t \tag{10}$$

where $\boldsymbol{v}$ are prediction errors $\boldsymbol{v}_t = \boldsymbol{y}_t - \mathbf{y}_{t|t-1}$. As such estimation of the model parameters $\boldsymbol{\theta}$ is possible by maximizing the likelihood function which consists of inputs obtained from running the Kalman filter.

The Kalman Smoother

When running the filter, the optimal estimate of the state vector at every point given information available at that point is obtained. To obtain more efficient estimates of the unobserved states at time t, the estimates can be conditioned on the entire information set and not just the information set available at time t. This is done with a *Kalman smoother*. There are multiple algorithms to obtain the smoothed estimates. I apply the *fixed-interval smoothing* algorithm, which is run after the Kalman filter, and iterates backwards through stored estimates of $\boldsymbol{a}_t$ and $\boldsymbol{P}_t$ as follows

$$\begin{aligned}
\boldsymbol{P}_t^* &= \boldsymbol{P}_t\boldsymbol{T}'\boldsymbol{P}_{t+1|t}^{-1} \\
\boldsymbol{a}_{t|T} &= \boldsymbol{a}_t + \boldsymbol{P}_t^*(\boldsymbol{a}_{t+1|T} - \boldsymbol{T}\boldsymbol{a}_{t+1}) \\
\boldsymbol{P}_{t|T} &= \boldsymbol{P}_t + \boldsymbol{P}_t^*(\boldsymbol{P}_{t+1|T} - \boldsymbol{P}_{t+1|t})\boldsymbol{P}_t^{*\prime}
\end{aligned}$$

B.2 Bayesian Estimation

Estimation and inference of unknown model parameters $\boldsymbol{\theta}$ in a Gaussian state space model is possible using maximum likelihood and the Kalman filter as seen above. It is also possible to obtain the optimal estimate of the unobserved states for every period through the Kalman smoother. The Kalman Smoother does not say anything about the underlying distribution of the states other than the mean, and inference on the obtained state estimates is therefore not possible. This challenge can be dealt with by applying Bayesian methods, which estimate the entire distribution of the unobserved states and parameters. Bayesian methods also

make it possible to include prior knowledge about parameters in the estimation, which can be useful in complex models, where maximizing the likelihood function may be challenging, or leads to extreme estimates as discussed in Harvey et al. (2007).

When applying a Bayesian approach distributions are derived from Bayes' theorem:

$$p(\boldsymbol{\theta}|\boldsymbol{y}) = \frac{p(\boldsymbol{y}|\boldsymbol{\theta})p(\boldsymbol{\theta})}{p(\boldsymbol{y})} = \frac{L(\boldsymbol{\theta}|\boldsymbol{y})p(\boldsymbol{\theta})}{p(\boldsymbol{y})}$$

where $p(\boldsymbol{\theta}|\boldsymbol{y})$ is the *posterior* distribution and $p(\boldsymbol{\theta})$ is the *prior* distribution, given by a belief about the distribution before estimating the model. The prior can also be chosen to be uninformative, such that prior beliefs don't affect the estimated posterior. $L(\boldsymbol{\theta}|\boldsymbol{y})$ is the likelihood and can be obtained from the Kalman filter for Gaussian models. $p(\boldsymbol{y})$ is known as the *marginal likelihood* and given by $p(\boldsymbol{y}) = \int_{\boldsymbol{\Theta}} p(\boldsymbol{y}|\boldsymbol{\theta})p(\boldsymbol{\theta})d\boldsymbol{\theta}$. The marginal likelihood is not available analytically, so the posterior distribution is unknown. To estimate the posterior distribution *Markov Chain Monte Carlo (MCMC)* methods can be used.

Markov Chain Monte Carlo

Markov Chain Monte Carlo is a broader class of algorithms that create a Markov chain of draws of $\boldsymbol{\theta}$. That is, the distribution of the current draw is given only be the previous draw. After a sufficient amount of draws, the distribution of the draws will match the true posterior probability distribution, which can be used for probabilistic inference. The coefficient estimates are then simply given by the mean of the draws and the 95% credible interval is between the 2.5th and 97.5th percentile of the draws. To obtain the Markov chain of draws the algorithms Metropolis-Hastings sampling and Gibbs sampling are typically used.

Metropolis-Hastings Sampling

In the Metropolis-Hastings algorithm a Markov chain is constructed by by drawing a proposed sample $\boldsymbol{\theta}_i^p$ based only on the previous sample $\boldsymbol{\theta}_{i-1}$ through a Markov transition density function $q(\boldsymbol{\theta}_i^p|\boldsymbol{\theta}_{i-1}) = q(\boldsymbol{\theta}_i^p|\boldsymbol{\theta}_{i-1}, ..., \boldsymbol{\theta}_0)$. The proposed draw is then accepted setting $\boldsymbol{\theta}_i = \boldsymbol{\theta}_i^p$ with probability γ, and rejected setting $\boldsymbol{\theta}_i = \boldsymbol{\theta}_{i-1}$ with probability $1 - \gamma$ where:

$$\gamma = \min\left(1, \frac{p(\boldsymbol{\theta}_i^p|\boldsymbol{y})q(\boldsymbol{\theta}_{i-1}|\boldsymbol{\theta}_i^p)}{p(\boldsymbol{\theta}_{i-1}|\boldsymbol{y})q(\boldsymbol{\theta}_i^p|\boldsymbol{\theta}_{i-1})}\right) \tag{11}$$

A better draw is therefore always accepted and a worse draw is accepted with some probability given by the relative fit of the draws. The marginal likelihood $p(\boldsymbol{y})$ cancels out of the fraction, and as such the probability of keeping a proposed draw is given by the likelihoods $L(\boldsymbol{\theta}|\boldsymbol{y})$, the priors $p(\boldsymbol{\theta})$ and the transition densities q which are all available. A common transition density is a random walk such that $\boldsymbol{\theta}_i^p = \boldsymbol{\theta}_{i-1} + \epsilon_i$. If ϵ is normally distributed, then $q(\boldsymbol{\theta}_i^p|\boldsymbol{\theta}_{i-1}) = q(\boldsymbol{\theta}_{i-1}|\boldsymbol{\theta}_i^p)$ and the transition densities cancel out of the fraction as well.

Gibbs sampling

Another method to obtain a Markov chain of draws is by Gibbs sampling which can be used if the *conditional distributions* of the elements of $\boldsymbol{\theta}$ are known. $\boldsymbol{\theta}$ consists of k unknowns, such that $\boldsymbol{\theta} = \{\theta^{(1)}, ..., \theta^{(k)}\}$. The conditional distributions are then

$$\begin{gathered} p(\theta^{(1)}|\boldsymbol{y}, \theta^{(2)}, \ldots, \theta^{(k)}) \\ \vdots \\ p(\theta^{(k)}|\boldsymbol{y}, \theta^{(1)}, \ldots, \theta^{(k-1)}) \end{gathered}$$

A Markov chain of draws is then achieved by sampling one θ-element at a time from the conditional distribution conditioned on all other newest draws:

$$\begin{aligned} \theta_i^{(1)} &\sim p(\theta_i^{(1)}|\boldsymbol{y}, \theta_{i-1}^{(2)}, \theta_{i-1}^{(3)}, \ldots, \theta_{i-1}^{(k)}) \\ \theta_i^{(2)} &\sim p(\theta_i^{(2)}|\boldsymbol{y}, \theta_i^{(1)}, \theta_{i-1}^{(3)}, \ldots, \theta_{i-1}^{(k)}) \\ &\vdots \\ \theta_i^{(k)} &\sim p(\theta_i^{(k)}|\boldsymbol{y}, \theta_i^{(1)}, \theta_i^{(2)}, \ldots, \theta_i^{(k-1)}) \end{aligned}$$

Metropolis-Hastings and Gibbs sampling can also be combined if the conditional distributions are only available for some subset of $\boldsymbol{\theta}$. Some subset of $\boldsymbol{\theta}_i$ is drawn using Metropolis-Hastings, and the rest are then drawn from their conditional distributions conditional on the newest draw of each θ.

Sampling Unknown Parameters and Unobserved States

In state space models the unknown model parameters $\boldsymbol{\theta}$ can be sampled using Metropolis-Hastings. For each draw of $\boldsymbol{\theta}$, the unobserved state vector $\boldsymbol{\alpha}$ can be sampled using Gibbs

sampling from the conditional distribution $p(\boldsymbol{\alpha}|\boldsymbol{\theta}_i, \boldsymbol{y})$. This is done using algorithms called *simulation smoothers*. The commonly used algorithm is presented in Durbin and Koopman (2002) and is given by:

1. Draw $\boldsymbol{\alpha}^+$ and $\boldsymbol{y}^+$ as:
   (a) Initialize $\boldsymbol{\alpha}_1^+ \sim N(\mathbf{0}, \boldsymbol{P}_1)$.
   (b) Iterate forwards through 4 and 6 to generate $\boldsymbol{\alpha}^+$ and $\boldsymbol{y}^+$.
2. Construct an artificial series $\boldsymbol{y}^* = \boldsymbol{y} - \boldsymbol{y}^+$.
3. Compute $\hat{\boldsymbol{\alpha}}^* = E(\boldsymbol{\alpha}|\boldsymbol{y}^*)$ by applying the Kalman smoother to $\boldsymbol{y}^*$.
4. Compute $\tilde{\boldsymbol{\alpha}} = \hat{\boldsymbol{\alpha}}^* + \boldsymbol{\alpha}^+$.
5. Then $\tilde{\boldsymbol{\alpha}}$ is a draw from $p(\boldsymbol{\alpha}|\boldsymbol{\theta}, \boldsymbol{y})$.

As the draws of $\boldsymbol{\theta}$ match the true distribution $p(\boldsymbol{\theta}|\boldsymbol{y})$, $\boldsymbol{\theta}$ is integrated out after enough draws: $p(\boldsymbol{\alpha}|\boldsymbol{y}) = \int_\Theta p(\boldsymbol{\alpha}|\boldsymbol{\theta}, \boldsymbol{y}) p(\boldsymbol{\theta}|\boldsymbol{y}) d\boldsymbol{\theta}$. When starting the Markov chain an initial $\boldsymbol{\theta}_0$ is chosen arbitrarily, and as such it can take some time for the chain to converge towards the true distribution. Therefore initial draws of θ are discarded. This is called the burn-in period. After the burn-in period the chain of draws should have converged and samples of $\boldsymbol{\theta}$ reflect the true distribution $p(\boldsymbol{\theta}|\boldsymbol{y})$ and draws of $\boldsymbol{\alpha}$ reflect $p(\boldsymbol{\alpha}|\boldsymbol{y})$. As such the entire distribution of the state vector for every period t is obtained when sampling the states, whereas only the mean of the distribution was obtained when directly applying the Kalman smoother.